DOI: 10.15669/pnst.7.371

Progress in Nuclear Science and Technology
Volume 7 (2025) pp. 371-376

ARTICLE

Development of a long-life laser ion source using a cryogenic solidified gas target

Yuji Inoue [a], Jun Hasegawa [a*], Naoki Matsubara [a], Kazumasa Takahashi [b], Jun Tamura [c], Kazuhiko Horioka [a] and Ken Takayama [d]

[a] Laboratory for Zero-Carbon Energy, Institute of Integrated Research, Institute of Science Tokyo, 2-12-1, Ookayama, Meguro-ku, Tokyo 152-8550, Japan; [b] Department of Electrical, Electronics and Information Engineering, Nagaoka University of Technology, 1603-1, Kamitomioka Nagaoka, Niigata 940-2188, Japan; [c] J-PARC Center, Japan Atomic Energy Agency, 2-4 Shirakata, Tokai-mura, Naka-gun, Ibaraki 319-1195, Japan; [d] High Energy Accelerator Research Organization (KEK), Accelerator Laboratory, 1-1 Oho, Tsukuba, Ibaraki 305-0801, Japan

We investigated the characteristics of a novel laser ion source using a cryogenic carbon dioxide (CO_2) target with the aim of applying it to next-generation heavy-ion cancer therapy accelerators. A cryogenic target was generated by depositing CO_2 gas on the surface of a cylindrical cold head cooled with liquid nitrogen. By irradiating the target with a frequency-doubled Nd:YAG laser, laser ablation plasmas containing up to C^{6+} ions were successfully generated and supplied with a peak current fluctuation less than ~5 %. It was also found that laser irradiation of cryogenic targets can damage not only the solidified CO_2 layer but also the copper substrate on the cold head due to the combined effects of laser ablation and shock wave propagation. Laser ablation experiments using a reproduced cryogenic target indicated that the reproducibility of plasma generation is gradually degraded with increasing number of the CO_2 layer reproductions due possibly to the deformation of the substrate. High-speed imaging was also performed to examine laser ablation and subsequent layer destruction processes, which reveals that the solidified CO_2 is fractured and removed locally around the laser spot and the damage area size depends on the layer thickness.

Keywords: Laser ion source; cryogenic target; solidified gas; heavy ion cancer therapy; laser ablation

1. Introduction

Heavy ion cancer therapy is a type of radiation cancer treatment using energetic carbon ions. Energetic heavy ions will locally deposit most of their kinetic energy just before they stop in the target (Bragg peak), so by using carbon ions with an energy of 200-430 MeV/u, we can damage cancer cells deep in the human body selectively compared to conventional radiotherapy using X-rays and γ-rays. However, because of the high construction cost of the heavy ion accelerator system, the spread of heavy ion cancer therapy particularly to developing countries is still on the way.

At present accelerator facilities for heavy ion cancer therapy, C^{4+} ions are usually generated by conventional plasma ion sources, such as electron cyclotron resonance (ECR) ion sources. After accelerated to several MeV/u by linear accelerators (injector), C^{4+} ions are converted to C^{6+} by a carbon thin film stripper and then injected to a radio-frequency (RF) synchrotron. To reduce the size and cost of the accelerator for heavy ion cancer therapy, Takayama, *et al*. have recently proposed a novel accelerator system based on the induction synchrotron technology, in which a laser ion source is used to supply about 4×10^8 high-charged carbon ions (C^{5+} and C^{6+}) directly to the synchrotron with a repetition rate of 10 Hz [1, 2].

Munemoto, *et al*. [3] and Fuwa *et al*. [4] have so far shown that highly ionized carbon ions are generated directly from graphite targets by laser ablation. These results mean that no injector such as RF linear accelerators is necessary in the accelerator system proposed here, leading to the large reduction of the size and cost of the heavy ion cancer therapy facility. On the other hand, it is known that when the graphite target in the laser ion source is repeatedly irradiated with the laser, damage accumulates on the target, making it difficult to reuse the target for subsequent plasma generation. Thus, one needs to replace the target on a regular basis, which limits the continuous operation time of the laser ion source.

To solve this problem, we propose to apply a solidified gas target to the laser ion source. Tamura, *et al*. successfully demonstrated plasma generation from a solidified neon/argon target formed on the 4-K cold head of a GM cryocooler, but the repetition rate of the plasma generation was limited to ~1 Hz due to the laser heat deposition on the cold head [5,6]. On the other hand, the cancer therapy machine proposed above requires 10-Hz operation of the laser ion source. Thus, the laser ion source developed in

*Corresponding author. E-mail: jhasegawa@zc.iir.isct.ac.jp

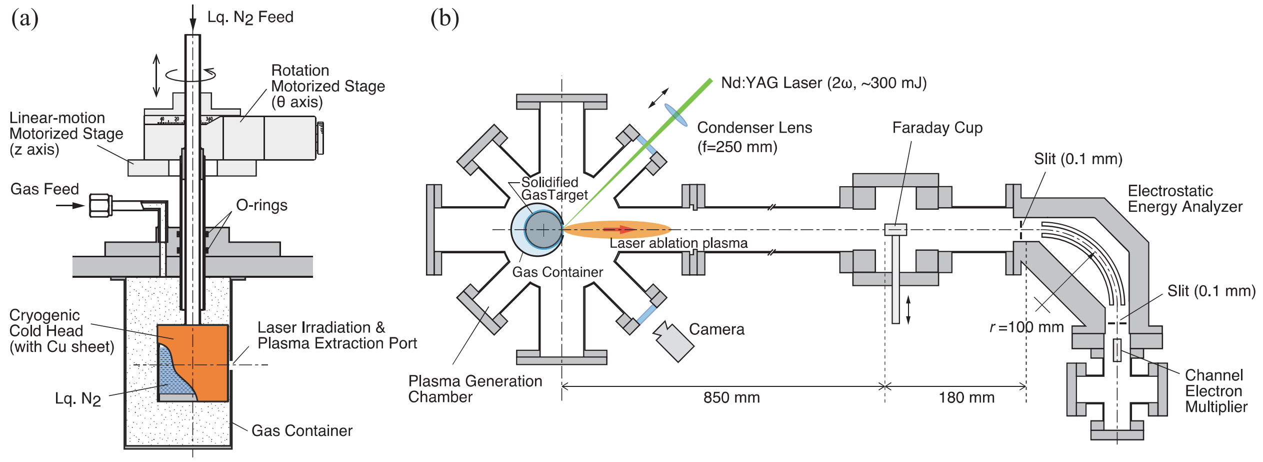

Figure 1. (a) Structure of cryogenic target, (b) an experimental setup for analysis of ions in laser ablation plasma.

this study adopts a mechanism that can replace the solidified gas target on the cold head for each laser shot; a thin solidified gas layer is formed on a cylindrical cold head, and plasma is generated by laser ablation while rotating the cold head in synchronization with laser irradiation. The solidified gas layer is locally destroyed and removed with each laser irradiation, but is reformed by deposition of continuously supplied "fuel" gas. This scheme allows us to continuously use the cryogenic target for a long operation time.

The final goal of this study is to develop a novel laser ion source using a reproducible solidified gas target and to demonstrate that it can operate stably without a limit on the target lifetime. This paper reports results of the first series of proof-of-principle experiments using a solid CO_2 target and describe the properties and reproducibility of plasmas generated by laser irradiation of cryogenic targets. Since some oxygen ions have the same mass-to-charge ratio as carbon ions and may contaminate the carbon beam, it is preferable to use oxygen-free gas. In the future, we plan to use oxygen-free hydrocarbon gas with a prototype device, but since safety measures against flammable gases are not yet sufficient, CO_2 gas was used in this series of proof-of-principle experiments.

2. Experimental setup

The cross-sectional side view of the newly developed cryogenic target is shown in **Figure 1(a)**. The target consists of a cryogenic cold head, a gas container, a gas supply system, and linear-motion and rotation motorized stages. The cold head is a stainless-steel cylindrical vessel with a diameter of 46 mm and a height of 50 mm. To protect the cold head from laser irradiation, a 100-µm thin copper sheet covers the side wall of the cold head. Liquid nitrogen is supplied to the cold head from a ø10-mm stainless-steel tube, which is supported by the motorized stages. The cold head is located in a stainless-steel cylindrical gas container with an inner diameter of 70 mm and a height of 115 mm. CO_2 gas is supplied from a gas cylinder to the container through a mass flow controller and exhausted through a ø10-mm hole in the side wall of the container. The azimuthal and vertical positions of the cold head inside the gas container are precisely controlled by the motorized stages. For heat insulation of the cold head, the ø16-mm stainless-steel support rod of the cold head has a vacuum insulation structure and the outer surface of the rod is sealed with O-rings.

A typical formation procedure of the cryogenic target (solidified CO_2 layer) is as follows. First, the background pressure around the cold head is evacuated to $\sim10^{-4}$ Pa. Then the surface of the cold head is cooled to ~88 K with liquid nitrogen. By feeding CO_2 gas with a flow rate of typically 25 sccm, a thin solid CO_2 layer is formed on the cold-head surface by deposition of CO_2. During the target formation, the cold head is continuously rotated with 1 rpm to improve the uniformity of the layer. Finally, when the layer thickness reaches a certain value, the gas supply is stopped.

Figure 1(b) shows the top view of the laser ion source test bench used in this study. The test bench consists of a plasma generation chamber, an ion flux measurement chamber, and an electrostatic energy analyzer. These chambers are evaluated to $\sim10^{-4}$ Pa by two sets of turbo molecular pumps. The cryogenic target is mounted in the plasma generation chamber so that the target surface is placed at the geometrical center of the chamber. A frequency-doubled Nd:YAG laser (300 mJ, 10 ns FWHM) is focused by a condenser lens (f=250 mm) onto the surface of the cryogenic target through a ø10-mm hole in the side wall of the gas container. A hot and dense plasma produced by laser ablation is extracted also through this hole. Because the solid CO_2 layer is partially destructed and removed by laser ablation, the cold head is rotated slightly between laser shots so that the laser can hit an undamaged area of the target.

In the present study the laser pulse energy was set to 300 mJ and the size of the elliptical laser spot on the cryogenic target was about 0.3 mm×0.7 mm. Thus, the averaged laser power density was $\sim2\times10^{10}$ W/cm^2. The fluctuation of the laser energy was less than 2.5%. The laser ablation plasma was measured 850 mm away from the target by a Faraday cup with an entrance aperture of ø5 mm. A bias voltage of -50 V was applied to the charge

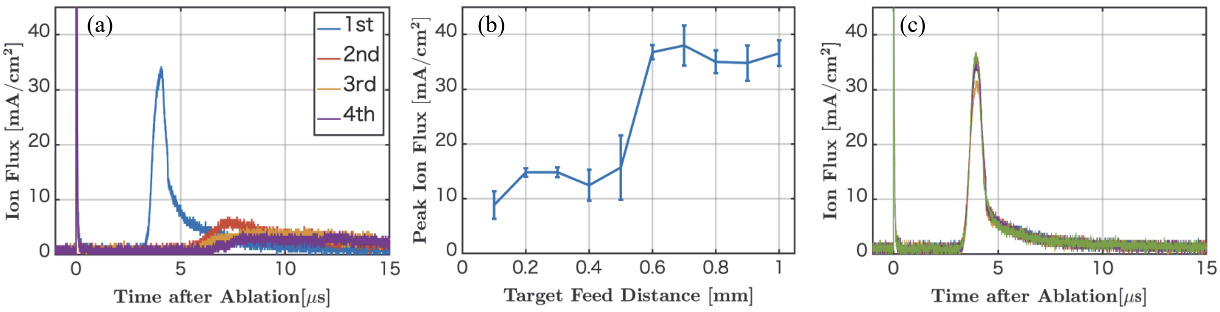

Figure 2. (a) Plasma ion flux waveforms obtained from a fixed laser irradiation position on the cryogenic target, (b) dependency of peak plasma ion flux on target feed distance, (c) typical plasma ion flux waveforms (5 shots overlaid) obtained with a target feed distance of 0.8 mm.

collector in the cup to detect only ions in the ablation plasma. The electrostatic energy analyzer was used for an ion-charge-state analysis. The analyzer is composed of two cylindrical deflection electrodes, entrance and exit slits (0.1 mm), and a channel electron multiplier (CEM) detector. Under a specific deflection voltage, only ions having a specific charge-to-mass ratio and a specific kinetic energy can be detected. We recorded detector signals by changing the deflection voltage from 15 V to 1500 V, and then reconstructed the flux waveform of ions in each charge state.

3. Results and discussion

Figure 2(a) shows plasma ion flux waveforms measured by the Faraday cup when the fixed position on the cryogenic target was repeatedly irradiated with the laser. The sharp impulse at $t = 0$ is the signal induced by intense light from the initial plasma generated during laser irradiation (~10 ns). Thus, the horizontal axis can be regarded as the flight time of ions traveling the distance (85 cm) from the target to the detector. In this measurement the total amount of supplied CO_2 gas was 50 cc (STP), corresponding to 2.2×10^{-3} mol. Assuming that the supplied CO_2 gas was uniformly deposited on the surface of the cold head, the areal density of CO_2 on the target was calculated to be 2.0×10^{-5} mol/cm^2. As shown in the figure, there is a significant difference between the waveform obtained by the first laser shot and those obtained by second, third, and forth laser shots. The first-shot plasma has a much larger and sharper peak than the others. In addition, the velocity of ions composing the first-shot plasma (~2×10^5 m/s) are considerably larger than those of the others. This result indicates that the first-shot plasma was composed of light element ions such as carbon and oxygen, while plasmas produced subsequent laser shots consisted mainly of heavy element ions such as copper, which are considered to have been ablated from the substrate. Therefore, it is natural to consider that the solid CO_2 layer within the laser spot on the target was completely removed by the first laser shot.

The above result indicates that the laser-irradiated CO_2 layer should be replaced with a fresh, undamaged one for subsequent laser shots. To investigate conditions for stable plasma generation with a cryogenic target, we measured the amount of plasma ion flux as a function of the target feed distance d_{tf}. Here, the target feed distance was defined as the distance between two successive laser irradiation positions on the target, and the target feed was achieved by stepwise rotation of the cylindrical cryogenic target. As shown in **Figure 2(b)**, the amount of generated plasma ions was strongly suppressed when $d_{tf} \leq 0.5$ mm. This is probably because local destruction of the CO_2 layer by the last laser shot directly affected plasma generation by the next laser shot. On the other hand, the peak plasma ion flux increased drastically as d_{tf} increased from 0.5 mm to 0.6 mm, and remained almost constant for larger d_{tf}. Typical plasma ion fluxes obtained when $d_{tf} = 0.8$ mm are shown in **Figure 2(c)**. From this result, we confirmed that stable plasma generation from the developed cryogenic target is possible with a flux fluctuation less than 5%.

A typical in-situ image of laser spots on the cryogenic target is shown in **Figure 3(a)**, which was taken at an interval between laser shots (Green light in the image is due to weak leakage light from the laser). Here, a couple of laser spots created by successive laser shots were observed from the ø10-mm hole of the gas container. In this measurement the target feed distance was set large enough so that the laser spots were separated. From the magnified image in **Figure 3(b)**, one can see that the laser spot consists of two distinct areas: a dark central area with a width of ~0.65 mm and a bright peripheral area with a width of ~1.2 mm. The same laser spot observed by a microscope in air is shown in Figure 3(c). Only the central dark region is visible in this image, and the copper substrate around it appears to be unchanged. Thus, this result indicates that the central area was formed directly by laser ablation process, while the peripheral area was formed by layer destruction due probably to a laser-driven shock wave. The image contrast between the laser-damaged peripheral area (without a CO_2 layer) and the undamaged area on the target (with a CO_2 layer) was likely enhanced by laser leakage light reflected by the smooth surface of the copper substrate. Since the solid layer formed by deposition of CO_2 gas has a relatively rough surface, diffused reflection weakened the laser leakage light, and the CO_2 layer was perceived as a relatively dark and matte image.

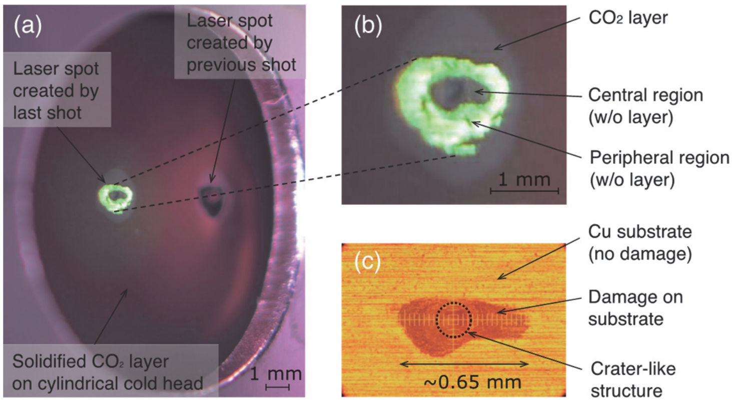

Figure 3. (a) An *in-situ* image of the cryogenic target observed from a 45º view port of the plasma chamber, (b) a magnified image of the laser spot in (a), (c) a magnified image of the laser spot observed in air.

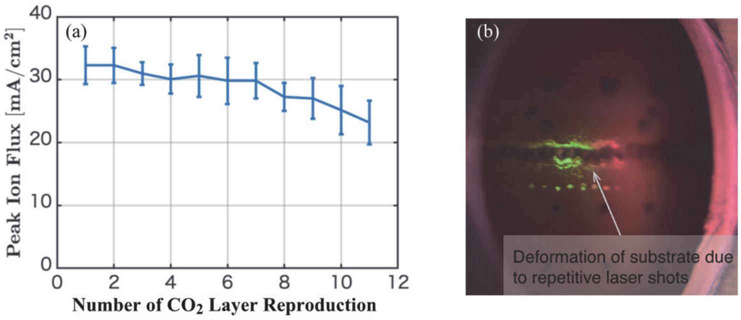

Figure 4. (a) Dependency of peak plasma ion flux on the number of CO_2 layer reproductions, (b) an *in-situ* image of the cryogenic target after 10-times CO_2 layer reproductions.

Careful observation of the image in Figure 3 reveals that the dark central area created by laser irradiation has a small crater-like structure with a diameter of ~0.2 mm and a maximum depth of ~5 µm. This is probably because the laser beam has a Gaussian-like intensity profile across the cross section. Since laser ablation is considered to have occurred more strongly in this crater region, the requirement for the target feed distance d_{tf} to achieve stable plasma generation should be given by:

$$d_{\mathrm{tf}} \geq (W_c + W_p)/2.$$

Here, W_c and W_p are the horizontal widths of the crater and the peripheral area defined in Figure 3, respectively. In the present experiment, d_{tf} is estimated to be (0.2+1.2)/0.2 = 0.7 mm, which well explains the result in Figure 2(b).

Figure 4(a) plots the peak ion flux as a function of the number of CO_2 layer reproduction. This data was obtained with a fixed vertical position and a target horizontal feed distance of 2.4 mm. In this condition, the cylindrical cryogenic target rotates ~360 degrees after 60 laser shots. We reproduced the CO_2 layer by supplying 100 cc of CO_2 gas each time the target rotated. The figure shows that the reproducibility of plasma generation degraded slightly with increasing number of layer reproductions, but the change in the peak plasma ion flux was well below the shot-to-shot variation with relatively small number of layer reproduction. However, when the number of reproductions exceeded seven, the averaged plasma ion flux decreased predominantly with each layer reproduction. This decrease is due possibly to the large deformation of the copper substrate. An *in-situ* image of the cryogenic target taken after 10-times layer reproductions is shown in **Figure 4(b)**. Apparently, the ablation damage accumulated on the target and the surface roughness of the substrate became remarkable. This substrate deformation might affect the uniformity of the reproduced CO_2 layer, which would have had a significant impact on the laser ablation process.

Figure 5(a) shows a typical signal waveform from the CEM detector in the electrostatic energy analyzer when the deflection voltage was 41.8 V. Note that the values on the horizontal axis in the figure were converted from time to mass-to-charge ratio of detected ions. By using the signal waveforms recorded with various deflection voltages from 15 V to 1500 V, we reconstructed flux waveforms of carbon ions having each charge state as shown in **Figure 5(b)** and **(c)**. To determine the signal intensity of each ion species, the peaks in the signal waveforms were separated from each other by fitting with Gaussian functions. These results show that carbon ions up to 6+ were successfully generated by laser ablation of solid CO_2. On the other hand, impurity ions such as hydrogen and oxygen were found to exist in the ablation plasma. When we inject C^{6+} ions to the accelerator,

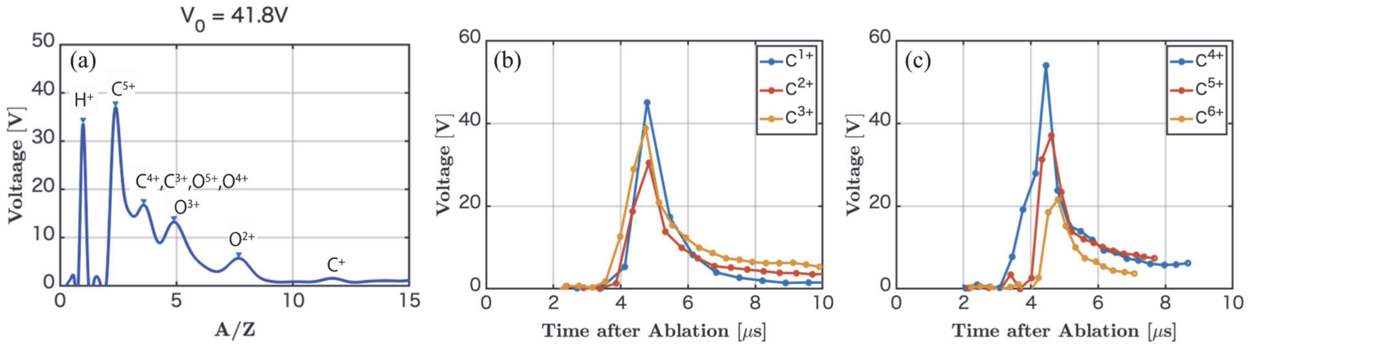

Figure 5. Reconstructed flux waveforms of carbon ions having different charge states from C^{+} to C^{6+}.

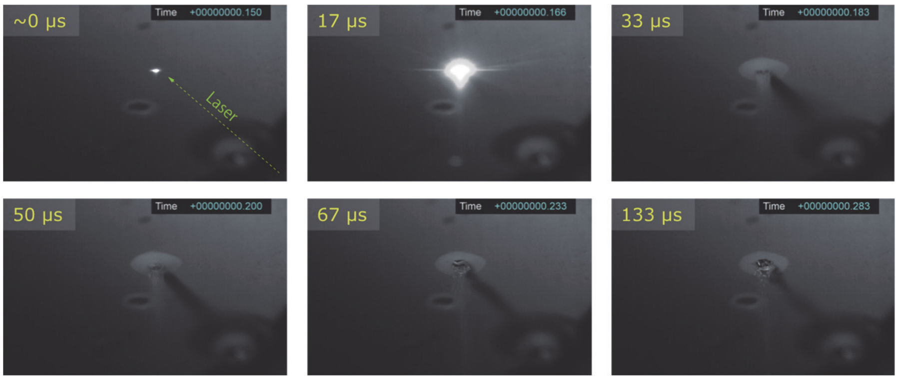

Figure 6. *In-situ* observation of CO_2 layer during laser ablation using a high-speed camera.

contamination of O^{8+} can be a problem because it is impossible to separate these two kinds of ions having the same charge-to-mass ratio. In this study, we focused to demonstrate high-charged carbon ion production by laser ablation of a solidified gas target and prove the concept of reproduction of the cryogenic target. Thus, we chose CO_2 gas from the safety reasons. In near future, we plan to use butane (C_4H_{10}) instead to avoid oxygen contamination. Since butane has higher sublimation temperature than CO_2, the formation of solid butane layer on the cryogenic head will be possible.

To investigate more in detail the behavior of the solid CO_2 layer after laser irradiation, we observed the surface of the cryogenic target with a high-speed camera. The images in **Figure 6** were taken with a frame rate of 60000 fps. The time on the upper left of each image denotes the elapsed time from the start of laser irradiation. In this measurement, the CO_2 layer of ~80 µm thick formed on the bottom of a cylindrical cold head was irradiated with a Nd:YAG laser (2ω) with an incident angle of 45 degrees. Right after the laser irradiation (t ~0 µs), strong light emission from the laser spot was observed in the first image, indicating that a hot plasma was generated and ejected into vacuum. Note that the exposure time per frame for this imaging was relatively long (~17 µs) and the second image in Figure 6 integrates all of the luminescence over this exposure time. Therefore, it is natural to consider that the bright emission in this frame is predominantly due to hot plasma within several microseconds after laser irradiation. At t = 33 µs, micro particles, probably finely crushed CO_2 crystal, were ejected from a hole drilled by the laser. Interestingly, a discolored circular area was observed around the hole, and the image taken 50 µs later showed that this area was slightly deformed downwards. Fragmentation of the solid CO_2 layer around the hole began ~67 µs later, and the final image (t =133 µs) shows that relatively large pieces of solid CO_2 were falling down due to gravity.

From these images, the destruction of the CO_2 layer seems to occur in two steps. The first step is just the laser ablation process, *i.e.*, the rapid heating of the CO_2 layer and the subsequent emission of a hot and dense plasma. This ablation process ends within a few microseconds at the most. In the second step, mechanical destruction of the CO_2 layer due to a laser-driven shock wave proceeds probably in the following manner: in the initial stage of the laser ablation, a strong shock wave is induced by ablation pressure toward the interior of the CO_2 layer and it propagates into the layer. The shock wave is partly reflected at the interface between the CO_2 layer and the substrate, and then propagates back to the layer surface. This shock propagation can induce many cracks in the CO_2 layer, eventually leading to local layer destruction.

It is clear that this local destruction of the cryogenic target by the shock wave cannot be avoided as long as the solidified gas target is used. The peripheral area observed in Figure 3 is exactly the result of plastic deformation of the CO_2 layer by the shock wave and subsequent fracture. However, if we can control the size of the peripheral area, this will not be a serious problem in the practical operation of the laser ion source. By determining the target feeding distance according to the peripheral area size, stable plasma production can be achieved as shown in Figure 2(c).

The laser ablation experiment in this paper used a relatively thin CO_2 layer with an areal density of ~2.0×10^{-5} mol/cm^2. From this value, the total amount of CO_2 molecules in a cylindrical volume defined by the laser spot size and the layer thickness is estimated to be 3.3×10^{-8} mol. Assuming that all these molecules evaporate, dissociate, and finally ionize to trivalent, they should consume at least 1.4 J of laser energy. This value is several times higher than the laser energy actually used in this study (~0.3 J). From this simple calculation and the well-known fact that not all of the laser energy is absorbed by the plasma, we should conclude that only a portion of solid CO_2 within the laser spot was converted to plasma in our experiments. Nevertheless, the solid CO_2 layer not only in the laser spot but also in the peripheral area was removed by the laser irradiation as shown in Figure 3. This fact shows that the layer destruction by the laser-driven shock wave dominates the consumption of the solidified gas target.

On the other hand, it is curious that laser irradiation marks remain clearly on the copper substrate. If the above calculation is correct, the laser ablation of the copper substrate should hardly occur. The results shown in Figure 2 strongly support this hypothesis. The so-called laser peening effect is thought to be one of the causes to create crater-like marks on the substrate. Possibly, the laser-driven shock wave locally exerted extremely strong pressure on the copper substrate, causing plastic deformation of it. The laser ablation experiment using a reproduced CO_2 layer (Figure 4) showed that the accumulation of substrate deformation can degrade the reproducibility of generated plasma. This is an issue that must be resolved in order to achieve long-time stable operation of the laser ion source. This problem could be greatly reduced by adopting harder substrate materials such as tungsten.

4. Conclusion

In this study, we developed a novel laser ion source adopting a reproducible cryogenic target to meet the demand for long-time supply of high-charged carbon ions at the heavy-ion accelerator facility for cancer therapy. In this proof-of-principle experiments, we succeeded in generating a solidified CO_2 layer on a cold head cooled with liquid nitrogen. Although the CO_2 layer was locally lost by a single laser irradiation, we found that the effect was limited to the small area around the laser spot. By setting the target feed distance properly, stable plasma generation from the solidified CO_2 was confirmed with a flux variation less than 5%. Charge state analyses revealed that carbon ions with charge states up to 6+ were produced and supplied by the developed laser ion source.

References

[1] K. Takayama, T. Yoshimoto, M. Barata, W. Kwee, L. Xingguang, T. Iwashita, S. Harada, T. Adachi, T. Arai, D. Arakawa, H. Asao, E. Kadokura, T. Kawakubo, H. Nakanishi, Y. Okada, K. Okamura, K. Okazaki, A. Takagi, S. Takao and M. Wake, Induction acceleration of heavy ions in the KEK digital accelerator: Demonstration of a fast-cycling induction synchrotron, *Physical Review Special Topics – Accelerators and Beams* 17 (2014), 010101.

[2] K. Takayama, T. Kawakubo, T. Adachi, T. Dixit and A. Shaikh, Energy-varying beam extraction assisted by large momentum deviation and charge exchange, *Physical Review Accelerators and Beams* 24 (2021), 011601.

[3] N. Munemoto, K. Takayama, S. Takano, M. Okamura and M. Kumaki, Development of the C6+ laser ablation ion source for the KEK digital accelerator, *Review of Scientific Instruments* 85 (2014), 02B922.

[4] Y. Fuwa, S. Ikeda, M. Kumaki, M. Sekine, N. Munemoto, D. Cinquegrani, M. Romanelli, T. Kanesue, M. Okamura and Y. Iwashita, Comparison of graphite materials for targets of laser ion source, *Review of Scientific Instruments* 85 (2014), 02B924.

[5] J. Tamura, M. Okamoto and T. Kanesue, Ion generation from a solidified Ne target for a laser ion source, *Applied Physics Letters* 91 (2007), 041504.

[6] J. Tamura, M. Okamura and T. Kanesue, Application of cryotarget to laser ion source, *Review of Scientific Instruments* 79 (2008), 02B101.